Apoptosis (2013) 18:271–285
DOI 10.1007/s10495-012-0798-y

ORIGINAL PAPER

Silica phagocytosis causes apoptosis and necrosis by different temporal and molecular pathways in alveolar macrophages

Gaurav N. Joshi · David A. Knecht

Published online: 18 January 2013

Abstract Chronic inhalation of crystalline silica is an occupational hazard that results in silicosis due to the toxicity of silica particles to lung cells. Alveolar macrophages play an important role in clearance of these particles, and exposure of macrophages to silica particles causes cell death and induction of markers of apoptosis. Using time-lapse imaging of MH-S alveolar macrophages, a temporal sequence was established for key molecular events mediating cell death. The results demonstrate that 80 % of macrophages die by apoptosis and 20 % by necrosis by clearly distinguishable pathways. The earliest detectable cellular event is phago-lysosomal leakage, which occurs between 30 and 120 min after particle uptake in both modes of death. Between 3 and 6 h later, cells undergoing apoptosis showed a dramatic increase in mitochondrial transmembrane potential, closely correlated with activation of both caspase-3 and 9 and cell blebbing. Externalization of phosphatidyl serine and nuclear condensation occurred 30 min–2 h after the initiation of cell blebbing. Cells undergoing necrosis demonstrated mitochondrial membrane depolarization but not hyperpolarization and no caspase activation. Cell swelling followed the decrease in mitochondrial membrane potential, distinguishing necrosis from apoptosis. All cells undergoing apoptosis followed the same temporal sequence, but the time lag between phago-lysosomal leakage and the other events was highly variable from cell to cell. These results demonstrate that crystalline silica exposure can result in either apoptosis or necrosis and each occurs in a well-defined but temporally variable order. The long time gap between phago-lysosomal leakage and hyperpolarization is not consistent with a simple scenario of phago-lysosomal leakage leading directly to cell death. The results highlight the importance of using a cell by cell time-lapse analysis to investigate a complex pathway such as silica induced cell death.

Keywords Silicosis · Apoptosis · Lysosome · Mitochondria · Caspase · Necrosis

Introduction

Silica, a naturally occurring inorganic mineral is an occupational hazard for miners, sand and granite workers, ceramic and brick workers and many others [1, 2]. Long-term inhalation of crystalline silica particles leads to silicosis, a potentially lethal disease that is marked by inflammation and fibrosis of the lung (IARC, 1997). Alveolar macrophages normally play a protective role in the lung by clearing foreign materials [3, 4]. There is substantial evidence that apoptosis of macrophages that take up silica particles plays a significant role in the etiology of silicosis [5, 6]. Upon continuous exposure to crystalline silica, a decrease in alveolar macrophage number was seen in vivo [7]. In vitro studies have shown that crystalline silica induces apoptosis in alveolar macrophages and cell lines. [8–10].

The effect of crystalline silica particles on cells that leads to the pathology associated with silicosis has been proposed to be related to oxidative stress [11, 12], cytokine

Electronic supplementary material The online version of this article (doi:10.1007/s10495-012-0798-y) contains supplementary material, which is available to authorized users.

G. N. Joshi · D. A. Knecht (✉)
Department of Molecular and Cell Biology, University of Connecticut, 91 N Eagleville Rd, Unit 3125, Storrs, CT 06269, USA
e-mail: david.knecht@uconn.edu

release [13–15] and excessive cell death mediated by apoptosis [8, 13, 16]. Apoptosis is a well-characterized process that can be initiated by various stimuli that activate either the extrinsic or the intrinsic pathway [17–20]. When alveolar macrophages are exposed to crystalline silica in vitro, the cells show a loss in mitochondria membrane potential and activation of caspases-9 and -3 [8, 11]. Furthermore when these cells were exposed to the pan-caspase inhibitor z-VAD-fmk before crystalline silica exposure, cell death was attenuated. Broncho-alveolar lavage fluid collected from mice instilled with crystalline silica also shows an increase in macrophage cell death. Mice administered with pan-caspase inhibitor zVAD-fmk show a reduction in macrophage cell death and the collagenous deposits indicative of fibrotic disease implicating apoptosis as one of the contributors to the progression of the disease [5]. Another mode of cell death is necrosis which is characterized by the swelling of a cell and release of its contents into the external milieu, thereby promoting inflammation [21, 22]. Necrosis has been measured in cells exposed to crystalline silica by an LDH release assay. Thus crystalline silica particle uptake and resultant cell death contributes to silicosis.

Thibodeau et al. [1, 2, 9] have outlined a process where in the earliest event to take place upon exposure of cells to crystalline silica is phago-lysosomal leakage with caspase activation at a later time. The authors did not attempt to provide a precise time-line of these events in a cell that has been exposed to crystalline silica particles. We have used time lapse imaging in conjunction with fluorescent reporter probes to map the temporal sequence of molecular events that occur in individual cells exposed to crystalline silica particles. We find that apoptosis and necrosis occur with distinct temporal sequences, but the time when events associated with either process occurs varies significantly from cell to cell. Single cell analysis has also revealed a novel transient hyperpolarization of mitochondrial membrane potential ($\Delta\Psi m$) at the initiation of apoptotic cell death. Furthermore, caspase activation, cell blebbing and hyperpolarization of mitochondria during apoptosis occur essentially simultaneously, but many hours after leakage of phago-lysosomes. During necrosis, swelling followed a rapid mitochondrial depolarization without any caspase activation.

Materials and methods

Cell culture

MH-S alveolar macrophages (ATCC CRL-2019) were maintained in RPMI-1640 media supplemented with 10 % FBS, HEPES, L-Glutamine and Ampicillin/Streptomycin (complete media). For live cell imaging 1.2×10^5 cells were plated in a 35 mm Bioptechs delta T glass bottom culture dish (Bioptechs, Butler, PA) with 1 ml complete media and allowed to adhere overnight at 37 °C in a 5 % CO_2 incubator.

Transfection

MH-S alveolar macrophages were transfected with DNA encoding the FRET probes CFP-IETD-YFP (initiator caspase-9 probe) [23] or CFP-DEVD-YFP (effector caspase-3 probe) [24] using Lipofectamine transfection reagent (Invitrogen). Briefly, 1.2×10^5 cells were plated overnight in RPMI complete media. 2 μg of DNA was used to transfect according to the manufacturers protocol. In order to obtain stably expressing cells, cells expressing the desired probe were selected by addition of G418 (1 mg/ml) for 48 h after which the media was replaced with RPMI complete media. Cells were allowed to grow and fluorescent colonies were directly picked from the culture dish manually with a pipette while viewing cells on the microscope stage.

Time-lapse imaging of physiological indicators of cell death

Crystalline silica (Min-U-Sil 5; US Silica, Berkeley Springs, WV) was baked at 83 °C for 18 h to remove any toxins and suspended at 2 mg/ml in CO_2 independent media (Invitrogen, Carlsbad, CA). Cells were plated in 35 mm Bioptechs dishes for 12 h in RPMI complete media. Depending on the assay, cells were incubated with an appropriate dye and imaged in CO_2 independent medium. Cells were treated with 50 $\mu g/cm^2$ crystalline silica by adding the suspended particles to the dish and allowing the particles to settle onto the cells.

Phago-lysosomal leakage was measured as an increase in the fluorescence of Fitc-dextran (4 and 70 kD, Sigma, St. Louis, MO). Media containing 1 mg/ml Fitc dextran (FD) was added to the cells and allowed to load by endocytosis in complete RPMI medium for 2.5 h. Cells were then washed with two changes with complete media and then cultured in CO_2 independent medium. Quantification of the leakage of FD was accomplished using a region of interest (ROI) in the nuclear region for 4 kD FD and over an entire cell for 70 kD FD.

Mitochondrial transmembrane potential ($\Delta\Psi m$), was measured using the potentiometric dye TMRE. In order to correlate the dynamics of caspase activation with changes in mitochondrial transmembrane potential ($\Delta\Psi m$), MH-S cells were plated in a Bioptechs dish and then incubated with 45 nM Tetramethyl rhodamine ester (TMRE, Invitrogen, Carlsbad, CA) for 20 min in complete media. After

20 min, the cells were washed two times with complete media and then 1 ml of CO_2 independent media without serum. To measure drug induced mitochondria hyperpolarization or depolarization, MH-S cells incubated with TMRE were treated with either 5 μg/ml oligomycin or 10 μM FCCP respectively and imaged every minute. To relate the timing of hyperpolarization to caspase activation, cells expressing either the initiator or the effector caspase FRET probe were labeled with TMRE as indicated above. FRET images were acquired at 30 min intervals for the first 4 or 5 h (minimal cell death was observed during this time) and then every 5 min for a total duration of 15 h. Variation in mitochondrial transmembrane potential was also assessed using Rhodamine-123 (10 μM) and similar results were obtained (data not shown). TMRE was used for the study as it has been reported to be less toxic and allows simultaneous imaging of caspase activation.

To determine when surface exposure of phosphatidyl serine (PS) occurs, 30 ng Annexin V-FITC (BD Biosciences, San Jose, CA) was added to cells cultured in CO_2 independent media. The probe was left in the medium throughout the experiment. This generated weak background fluorescence, but the concentration of the probe at the membrane of apoptotic cells was easily visualized above this background. Cells were then exposed to 50 μg/cm^2 crystalline silica and DIC and fluorescence images captured every 30 min.

Changes in nuclear morphology and nuclear condensation were analyzed using the vital nuclear dye Hoechst 33342. Cells plated in complete RPMI medium were incubated with 5 μg/ml Hoechst 33342 for 30 min, washed two times with complete medium and then cultured in CO_2 independent medium. DIC and fluorescence images were taken every 30 min. This stained the nuclei that remained fluorescent throughout the experiment.

Imaging and image analysis

For live cell imaging, Bioptechs dishes were mounted in a Delta T holder on the stage of a Zeiss Axiovert 200 M widefield fluorescence microscope and the temperature was maintained at 37 °C with a Delta T controller and heated lid. Imaging was done using 63× Plan Apochromatic 1.4 NA oil immersion lens and a Hamamatsu ORCA-ER camera (Hamamatsu, Bridgewater, NJ). Images were acquired using time-lapse automation modules in OpenLab software (Perkin-Elmer, Waltham, MA). FRET imaging was done using a CFP-YFP FRET filter set with excitation at 436 nm and emission at 480 and 535 nm respectively. TMRE imaging was done using 562 nm excitation and 624 nm emission. Fitc-dextran was imaged using a GFP filter set and Hoechst-33342 with a DAPI filter set. Both DIC and fluorescence images were captured at each time point and image processing and analysis was done using Image J [25]. TMRE fluorescence was measured by drawing a ROI around a cell and measuring mean fluorescence. Background fluorescence value of media was subtracted from mean fluorescence. For FRET ratio measurements, mean pixel intensity from CFP and FRET channels for a single cell were obtained by drawing a ROI around a cell at each time point and measuring the mean fluorescence. The CFP/YFP ratio was obtained by exporting these values to Excel (Microscoft Corporation, Redmond, WA) and graphs were made using Prism (Graphpad Inc, La Jolla, CA). To generate ratiometric images, the Ratio plus plugin for ImageJ was used to divide the CFP image set by the FRET image set. The spectrum look up table was assigned to the resultant CFP/YFP images.

Cells labeled with TMRE were also imaged by confocal microscopy. Cells were labeled with TMRE as described above and imaged in a Bioptechs dish in a Delta T holder on the stage of Leica confocal microscope. Imaging was done using a 40× Plan Apochromatic 1.25 NA oil immersion lens with 543 nm excitation. A stack of seven z-slices, 2.3 μm apart was captured at 5 min intervals for a total of 10 h.

Results

Phago-lysosomal leakage starts within 30 min of crystalline silica treatment

Thibodeau et al. [3, 4, 9] have shown leakage of Fitc-dextran (FD) from endosomes into the cytoplasm within 1 h of crystalline silica treatment. To determine more precisely the time when leakage occurs and the size of the pores through which molecules can pass into the cytoplasm, cells were pre-loaded with either 4 or 70 kD FD and then imaged over time after addition of crystalline silica particles. Leakage of both 4 kD FD (Fig. 1a) and 70 kD FD (Fig. 1b) could be seen within 30 min following crystalline silica addition. With 4 kD FD there was an increase in both cytoplasmic and nuclear fluorescence, consistent with the cutoff limit for passive diffusion through nuclear pores [26]. In cells loaded with 70 kD FD, there was labeling of the cytoplasm, but not the nucleus. Since not all vesicles leak, quantification of the cytoplasmic fluorescence increase could be affected by the presence of intact vesicles. This problem was minimized by the increased emission from fluorescein as it moved from acidic vesicles to the more neutral cytoplasm. In cells loaded with 70 kD FD, a detectable increase in the FITC fluorescence around the crystalline silica particles was also observed at 45 min (Supplementary Fig. 1c, d arrows).

This is likely to be due to an increase in the pH of phagolysosomal compartments arising from equilibration of the contents with the cytoplasm as the vesicles become permeabilized. A measurable increase in cytoplasmic fluorescence could be detected as early as 30 min after crystalline silica addition (Fig. 1c, d).

The time of initiation of FD leakage varied from cell to cell. Cells were seen leaking as early as 30 min but some cells took as long as 135 min to begin leaking (Supplementary Fig. 1a, b). The data show a gradual increase in cytoplasmic FITC fluorescence over time in all cells and eventual plateauing of the signal. At this point, no more punctate vesicles were observed in the cells indicating that either the entire endo-lysosomal compartment has become permeabilized or the cytoplasmic fluorescence is too high to visualize them. Averaging over many cells shows that leakage occurred over a 2 h period, starting about 30 min after crystalline silica addition (Fig. 1e). From the same set of data, individual cells were quantified based on the time that leakage was initiated (Fig. 1f). This clearly demonstrates the variability in the timing of leakage with 60 % of the cells leaking between 60 and 105 min.

Apoptotic cells undergo transient hyperpolarization of mitochondria

Mitochondria are key players in events leading to cell death by apoptosis [5, 6, 10, 27]. Some changes in mitochondrial function have been found following crystalline silica treatment using approaches which provide an average value for an asynchronous population of cells [7, 8, 11]. For our single cell time-lapse approach, cells were loaded with the potentiometric cationic dye TMRE and then exposed to 50 μg/cm^2 crystalline silica and imaged over time. There was little change in fluorescence for about 5 h and then the fluorescence signal from individual cells would rapidly increase (hyperpolarization) and then slowly decrease until they reached a background level characteristic of depolarized mitochondria (Fig. 2a). The cells that showed hyperpolarization were simultaneously observed to be undergoing membrane blebbing in the DIC channel (Supplementary movie 1). The time at which cells began to show hyperpolarization was quite variable, ranging from 330 to 1,100 min (Fig. 2b).

Hyperpolarization is not a commonly observed feature of the apoptotic cell death pathway. In order to verify that the hyperpolarization was due to an increase above normal ΔΨm and not an artifact of unquenching of TMRE, cells were treated with oligomycin, an F_1–F_0 ATP'ase (complex V) inhibitor of oxidative phosphorylation. This compound prevents protons from getting pumped back into the matrix space, resulting in hyperpolarization of mitochondria [8–10, 28, 29]. When TMRE labeled MH-S cells were treated with oligomycin, there was an increase in TMRE fluorescence within 1 min (Fig. 2c, e; Supplementary movie 2). To test the sensitivity of TMRE towards loss of ΔΨm, FCCP, a nonspecific protonophore and uncoupler of oxidative phosphorylation, was added to cells loaded with TMRE [11, 12, 29]. Upon addition of FCCP, TMRE fluorescence decreased immediately indicating mitochondrial depolarization (Fig. 2d, f; supplementary movie 3). To confirm that the increase in TMRE fluorescence observed with widefield imaging was not due to an increase in the local concentration of TMRE or due to aggregation of mitochondria during cellular contraction, multi-plane confocal imaging was performed. An increase in TMRE fluorescence was also observed in these images (Supplementary Fig. 2). Thus cells go through a period in which mitochondrial function is altered to generate excessive transmembrane potential before they become depolarized.

Apoptotic cells undergo nearly simultaneous mitochondrial hyperpolarization, caspase activation and membrane blebbing

Crystalline silica exposure has been shown to cause activation of both caspase-9 and 3 in alveolar macrophages [8, 11, 13–15]. The temporal relationship between changes in mitochondrial membrane potential (ΔΨm) and caspase activation or changes in cellular morphology during apoptosis has not been examined. To relate the timing of mitochondrial changes to other apoptotic events, MH-S cells stably expressing either initiator (caspase 9) or effector (caspase 3) FRET reporter probes were isolated [8, 13, 16, 23, 24]. These cells were loaded with TMRE and then the cells were exposed to crystalline silica particles and imaged over time. An example of the progression of events is shown for a single cell in Fig. 3. No alterations in the probes were observed for about 5 h after crystalline silica particle addition (Fig. 3a; Supplemental Movie 4). At 335 min, the cell retracted and by 340 min started to bleb (Fig. 3a, DIC). At the same time, the TMRE fluorescence signal increased dramatically and the caspase-9 FRET reporter CFP/YFP ratio increased, indicative of caspase-9 activation (Fig. 3a). Mitochondrial hyperpolarization persisted for 15 min and then the ΔΨm decreased until the mitochondria were depolarized. Quantitative analysis of TMRE and FRET signals shows the extremely narrow window of time in which these two events are initiated (Fig. 3b). The first image where there was an increase in FRET ratio was also the first time point where there was a detectable increase in mitochondrial membrane potential. Since images were taken 5 min apart, this implies that the two events happen within 5 min of each

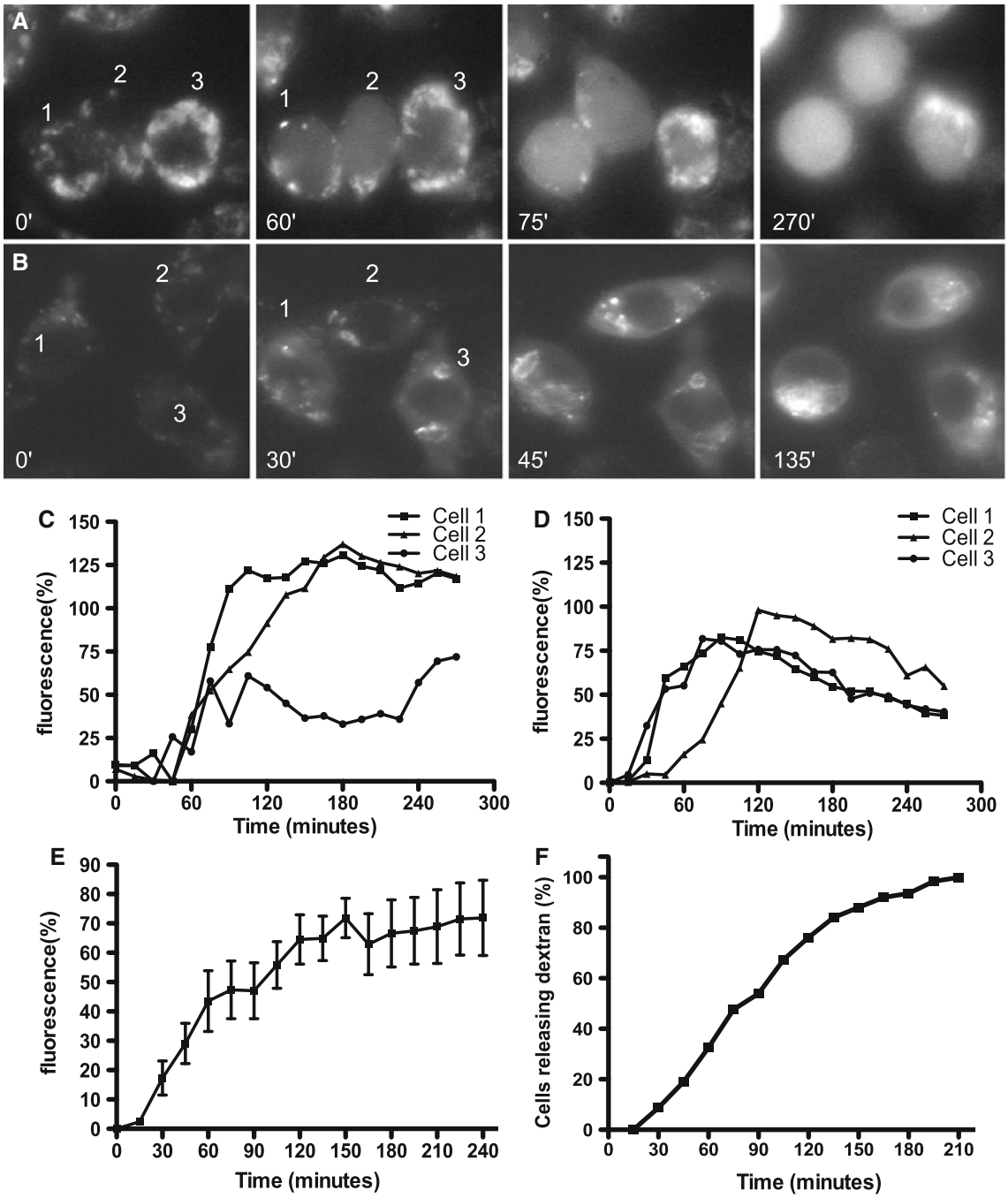

Fig. 1 Phago-lysosomal damage is the earliest injury to occur after crystalline silica treatment. MH-S cells were loaded for 2.5 h with either 4 or 70 kD Fitc-dextran (FD) to label endo-lysosomal compartments. Both probes initially label small punctate vesicles (0 time images). **a** After crystalline silica addition, 4 kD FD moves to both the cytoplasmic and nuclear compartments, **b** whereas 70 kD FD is only found in the cytoplasm. The fluorescence increase was quantified as percent increase over the time with respect to 0 h in the nuclear region for **c** 4 kD FD and the whole cell for **d** 70 kD FD. **e** Phago-lysosomal leakage occurred, began to increase between 15 and 30 min and continued until plateauing about 120 min later. Data is represented as a mean of percent increase in the fluorescence intensity ±S.E.M from 10 separate experiments. **f** From these 10 experiments, individual cells were analyzed for the time at which they first show an increase in fluorescence over background indicating the start of leakage. Although leakage began within 30 min in some cells, 60 % of cells show leakage between 60 and 105 min

other (Fig. 3c). Both events were also closely correlated with the start of cell membrane blebbing (Supplementary movie 4).

A similar analysis was carried out to analyze the timing of effector caspase-3 activation relative to changes in the TMRE fluorescence and cell blebbing (Fig. 4a;

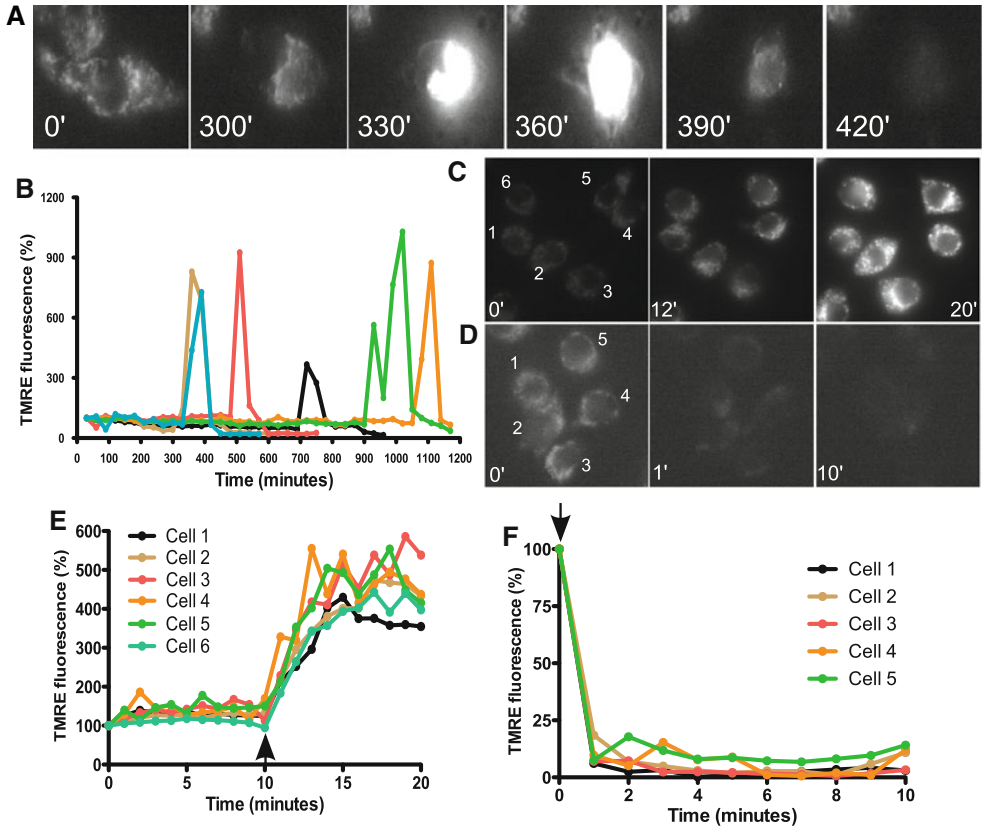

Fig. 2 Mitochondria become hyperpolarized in cells exposed to crystalline silica particles. Cells treated with TMRE were exposed to crystalline silica particles and imaged every 30 min to detect changes in mitochondria membrane potential (ΔΨm). **a** Shows a single cell that undergoes an increase in TMRE fluorescence at 330 min (hyperpolarization). **b** Is the quantification of TMRE fluorescence from 6 different cells over time after crystalline silica treatment. **c** Confirmation that mitochondrial hyperpolarization was not due to TMRE unquenching was obtained by treating cells with F_1–F_0 ATP'ase inhibitor oligomycin, which caused a gradual increase in TMRE fluorescence. **f** Quantitative data for these six cells represents this trend. Mitochondrial depolarization was confirmed by adding FCCP, a protonophore and uncoupler of mitochondrial oxidative phosphorylation. Cells immediately lose their fluorescence upon addition of FCCP (D). **g** Quantitative data for these five cells represents this trend. All images were captured at 1-min interval. *Arrows* in charts f and g indicates addition of oligomycin and FCCP respectively

Supplementary movie 5). At 690 min the cell retracted and at 750 min began to bleb. Both the TMRE signal and the FRET ratio also began to increase at 750 min. Quantitative analysis of images confirms that the increase in hyperpolarization and effector caspase activation occurred in the same narrow time window (Fig. 4b, c).

In both two cases shown above, cell morphology, ΔΨm and caspase activity occurred at the same time, but very different times relative to when crystalline silica was added. In order to determine the consistency of this sequence of events, this analysis was extended to include cells from multiple experiments (Fig. 5 and data not shown). In each case, there was an overlap in the timing for initiator (Fig. 5a) or effector (Fig. 5c) caspase activation with an increase in ΔΨm (Fig. 5b, d) and blebbing. Although these events started at the same time, the time when the events occurred relative to when crystalline silica was added varied dramatically between cells, ranging from 300 to 775 min. Thus there is a difference in the time that each cell takes to initiate the changes associated with apoptosis, but every cell shows a similar critical time at which blebbing, mitochondrial hyperpolarization and caspase activation occurs.

Cells undergoing apoptosis are Annexin V positive and undergo chromatin condensation

Phosphatidylserine (PS) flipping to the outer leaflet of the membrane and changes in nuclear morphology are commonly used as markers for detecting apoptotic cells [17–20, 30, 31]. We used Annexin V-FITC as a marker of PS flipping to determine when this event occurred relative to blebbing and caspase activation. Cells were incubated in a low concentration of Annexin V-FITC following crystalline silica addition and imaged over time. At this low concentration, the concentrating effect of binding the probe to the membrane upon PS flipping produces a cell-associated signal much greater than the background from

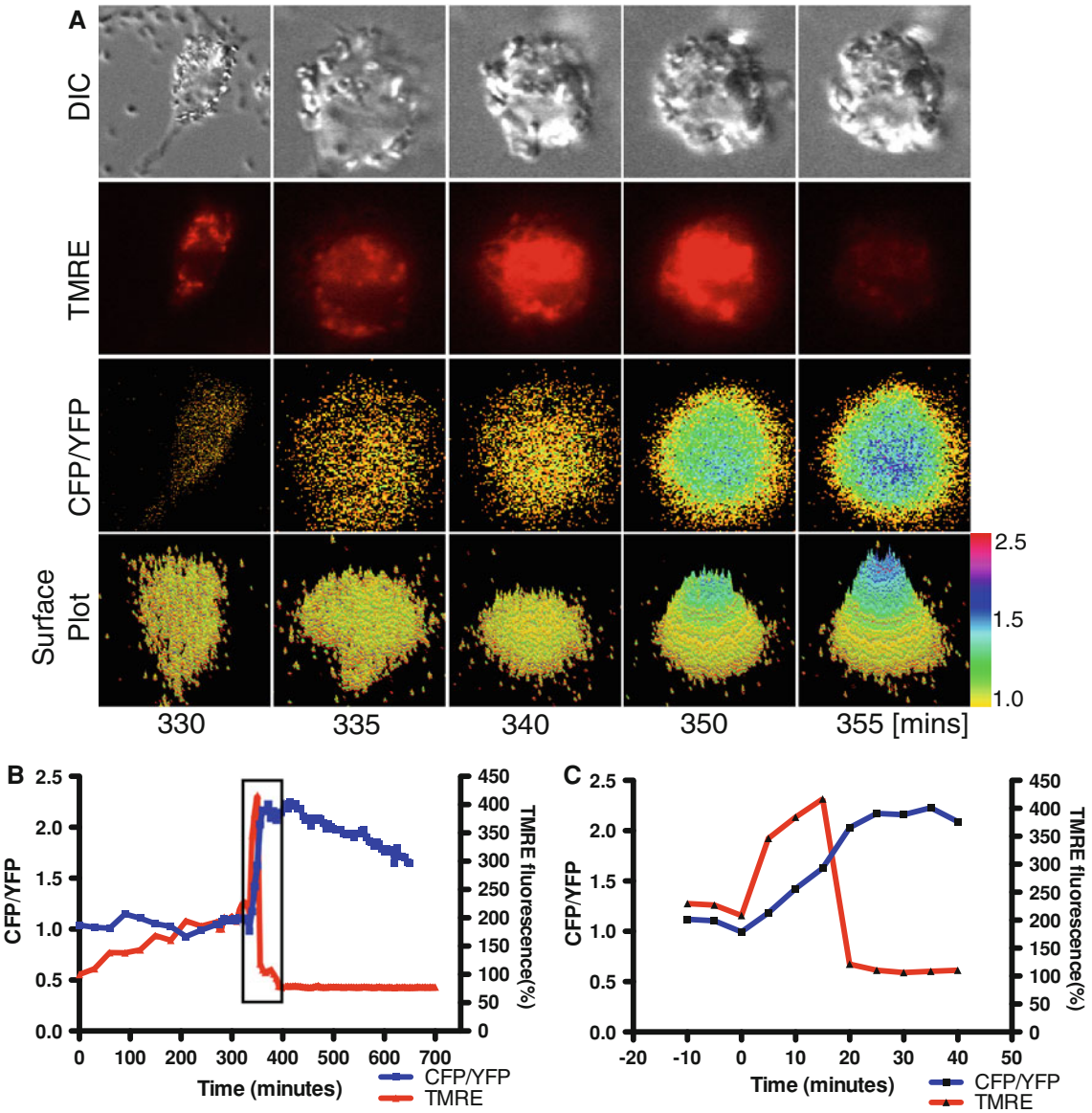

Fig. 3 Initiator caspase activation occurs at the same time as mitochondrial hyperpolarization and cell blebbing MH-S cells transfected with the Caspase 9-FRET probe were labeled with TMRE, exposed to 50 μg/cm^2 of crystalline silica and then imaged every 30 min for 270 min and then every 5 min until the end of the experiment. **a** At 330 min the cell was flattened and elongated with punctate mitochondrial fluorescence. It then rounded up at 335 min and began to bleb at 340 min. At the same time there was an increase in the TMRE fluorescence indicative of mitochondrial hyperpolarization and caspase activation that can be seen in the series of pseudo colored CFP/YFP and a surface plot of the data. **b** Quantitative analysis of mitochondrial membrane potential and caspase activation shows that the events occur at the same time within the temporal resolution of the experiment (5 min). The caspase probe continues to increase for 150 min and then plateaus. Blebbing begins at the same time point where the other probes first show an increase. **c** *Rectangular box* in **b** is expanded in **c** with time 0 as a time point that precedes cell blebbing

the media. Cells undergoing apoptosis show bright fluorescence around the cell membrane after they have started to bleb (Fig. 6a; supplementary movie 6) Analysis of individual cells shows a temporal variation in PS flipping relative to membrane blebbing (Fig. 6b), however the sequence of events for every cell is still the same; a cell retracts, blebs and later becomes Annexin V positive while continuing to bleb. On average, it took 70 min after the start of blebbing for cells to become Annexin V positive.

Chromatin condensation has also been reported for cells undergoing apoptosis. Cells were loaded with vital nuclear dye Hoechst 33342 to visualize nuclei. Hoechst 33342 was found to be toxic to cells if they were frequently exposed to UV light so the imaging interval was increased to 30 min. Upon crystalline silica

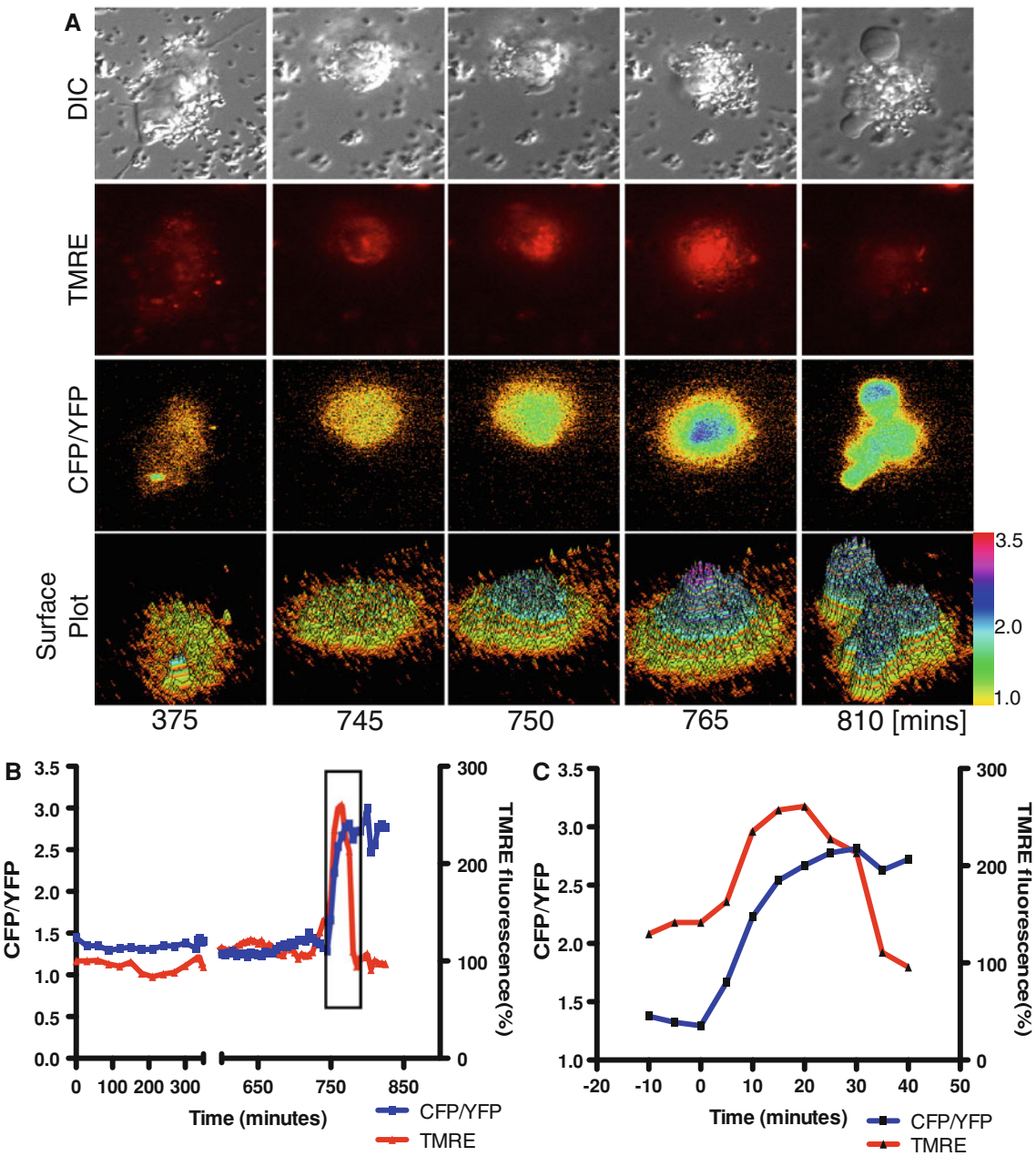

Fig. 4 The timing of effector caspase activation relative to mitochondrial potential and cell morphology MH-S cells expressing Caspase-3- FRET probe were incubated with TMRE, exposed to 50 μg/cm^2 of crystalline silica and imaged every 30 min for 330 min and then every 5 min till end of the experiment. **a** DIC, TMRE and CFP/YFP images represent any changes in cell morphology, mitochondrial physiology and FRET changes respectively. At 375 min a cell that was flat and elongated. The cell began to round up at 690 min and at 750 min cell began to bleb. At the same time, mitochondrial hyperpolarization and an increase in FRET ratio was detected. The mitochondrial hyperpolarization was sustained for 35 min and at 780 min the cell began to show a decrease in TMRE fluorescence indicative of mitochondrial depolarization. The data is also represented as surface plot that generates 3D view of the FRET ratio increase in a cell. **b** Quantitative analysis of the images shows both mitochondrial hyperpolarization and caspase activation occur in close temporal proximity. **c** *Rectangular box* in **b** is the region magnified in this graph with time 0 as a time point that precedes cell blebbing

treatment, no change in the nuclear morphology was observed until cells started to bleb. Chromatin condensation was observed approximately 60 min after blebbing for cells undergoing apoptosis (Fig. 6c; Supplementary movie 7).

A small fraction of cells undergo necrosis after crystalline silica treatment

Necrosis is another mode of cell death wherein a dying cell loses mitochondrial membrane potential, swells and then

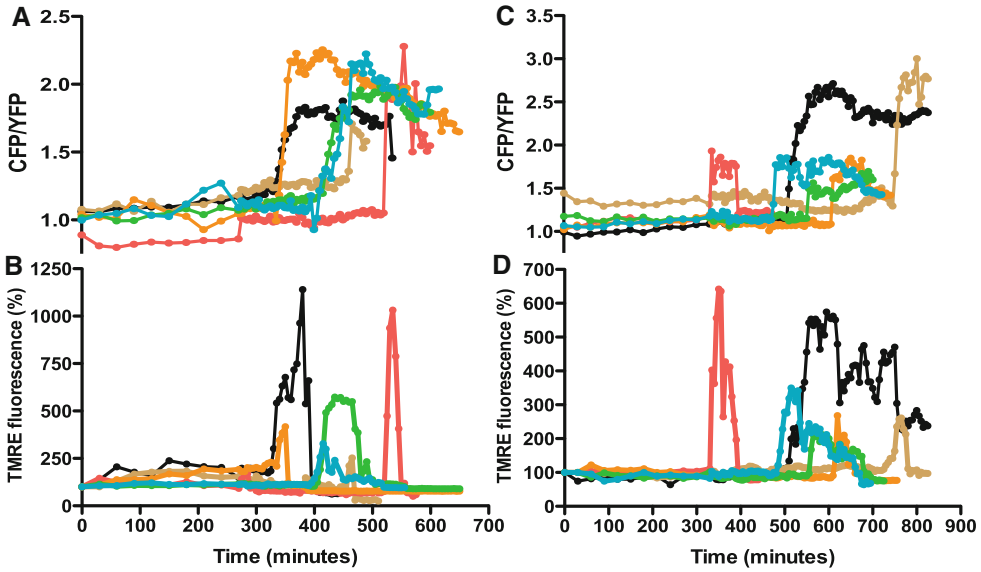

Fig. 5 Hyperpolarization and caspase activation occur at the same time in crystalline silica treated cells. Quantitative analysis of six representative cells labeled and imaged as in Figs. 3 and 4. Cells expressing **a** the initiator caspase probe or **c** the effector caspase probe and **b** and **d** labeled with TMRE respectively show an intercellular variation in the timing of events. However, in each cell, the increased TMRE fluorescence and FRET ratio occur at the same time. Individual trend lines representing data for a single cell are depicted with the same color. The same phenomenon was observed in all cells analyzed for initiator (n = 15) and effector caspase (n = 23) activation

its contents begin to leak out. In the same population of crystalline silica treated cells that died by apoptosis, about 15 % of cells died by necrosis (Fig. 7c). Cells undergoing necrosis did not bleb, show caspase activation or undergo mitochondrial hyperpolarization. Instead, they began to swell (Fig. 7a, DIC), lose mitochondrial $\Delta\Psi m$ (Fig. 7a, TMRE) and show no increase in the caspase reporter FRET ratio (Fig. 7a and b). The observed decrease in the CFP/YFP ratio is likely due to leakage of the cytoplasmic contents. Necrosis was more variable than apoptosis, occurring as early as 2 h after crystalline silica addition and as late as 10 h. AnnexinV-FITC staining was not observed in cells undergoing necrotic cell death (Fig. 7d). Also, in cells undergoing necrosis, nuclear condensation as observed by Hoechst 33342 did not take place and there was no change in nuclear morphology (Fig. 7e). Thus some cells undergo necrosis after silica treatment, but the molecular pathway is clearly distinguishable from the apoptotic pathway.

Temporal events during crystalline silica induced cell death

Integrating data from all the experiments we are able to establish a molecular pathway of events leading to cell death by either apoptosis or necrosis upon crystalline silica exposure to MH-S macrophages (Fig. 8). The earliest apoptotic event that we can detect is the leakage of phagolysosomal compartments beginning around 30 min after exposure of cells to crystalline silica particles. Within 2 h of the start of leakage, no punctate vesicular fluorescence can be seen. Although this leakage begins as early as 30 min after crystalline silica addition, the downstream activation of initiator and effector caspases as well as the increase in mitochondrial membrane potential were not seen for at least another 3 h. The timing varies dramatically from cell to cell, but the pattern of events is very reproducible. Cell blebbing, an increase in mitochondria membrane potential and initiator and effector caspase activation all occured at the same time. PS externalization and changes in nuclear morphology were observed to occur 30 min–2 h after the initiation of cell blebbing. Eventually these cells underwent secondary necrosis in which they swelled and mitochondria depolarized. In cells undergoing necrosis, cells swell and mitochondria depolarize without any change in caspase activity, PS flipping and chromatin condensation.

Discussion

Studies showing apoptosis or necrosis as a model of cell death leading to fibrosis have provided little information regarding the extent of coexistence of both types of cell death in cells exposed to crystalline silica. We have previously shown that MH-S macrophages phagocytose crystalline silica particles within 15 min of their exposure and that internalization of a single particle is sufficient to cause

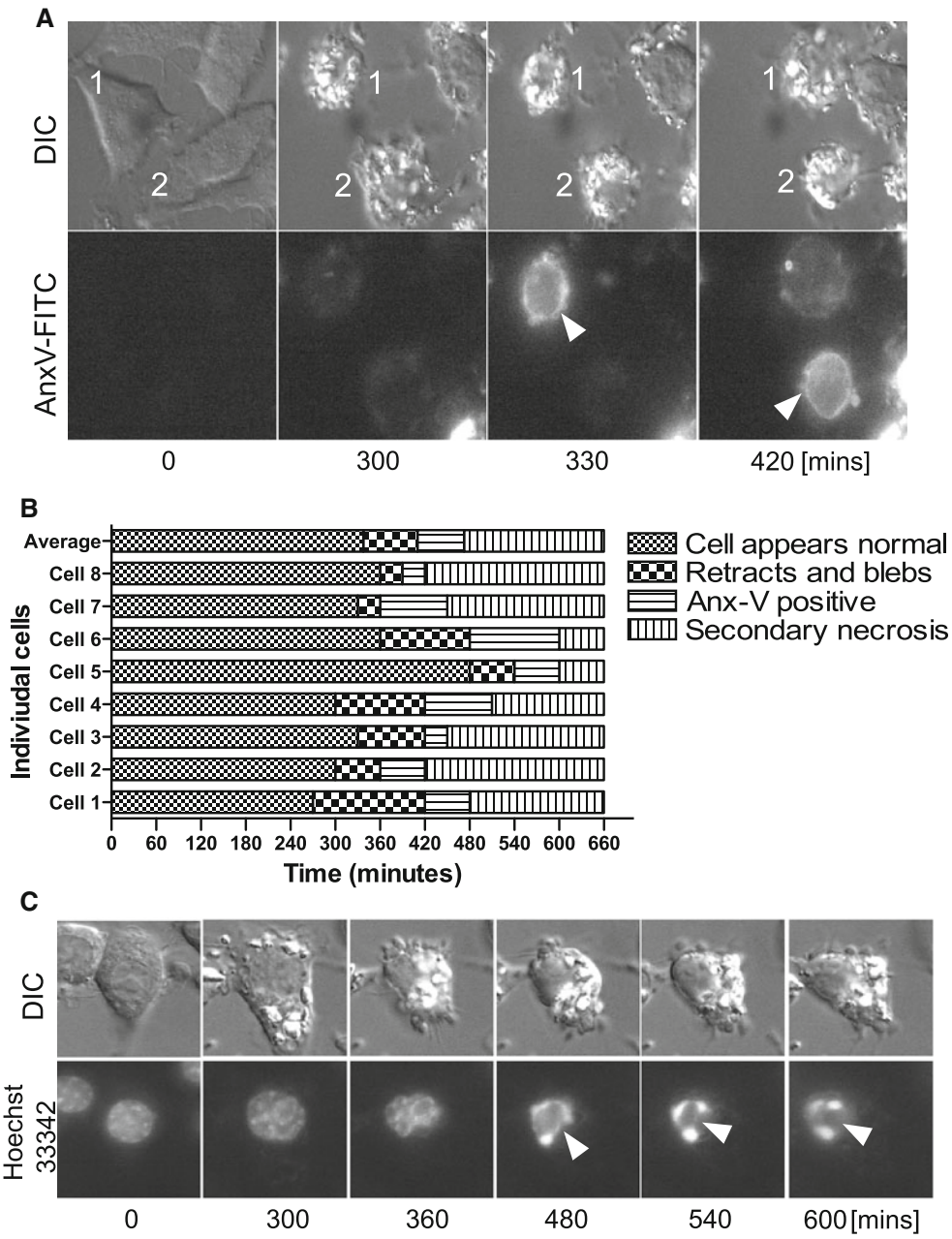

Fig. 6 Cells undergoing apoptosis show phosphatidyl serine exposure and nuclear condensation. **a** Cells were incubated with Annexin V-FITC and then exposed to crystalline silica particles. Annexin V-FITC fluorescence was seen only after the cells started to bleb. DIC images for cell 1 show rounding and blebbing at 300 min where as corresponding Annexin V-FITC fluorescence is observed after cell starts to bleb at 330 min as marked by arrow. Similarly, although, Cell 2 shows blebbing at 330 min (DIC), no visible AnnexinV-FITC fluorescence was seen till 390 min. **b** Comparison of the timing of AnnexinV-FITC binding versus morphological changes in the cell. There is variation in when blebbing and PS exposure occurs, but the order of events is the same in each cell. **c** Cells were incubated with Hoechst-33342 and imaged every 30 min to visualize any changes in the nucleus upon crystalline silica exposure. There was no change in the nuclear morphology until well after cell blebbing. Cells showed nuclear condensation 30–60 min after blebbing began

cell death [8, 11, 32, 33]. Here we examine the molecular pathway leading to cell death. The particles enter the cell in a phagosome, which subsequently undergoes maturation and fuses with lysosome to become a phago-lysosome. Since uptake of latex particles does not cause cell death, and crystalline silica particles are not broken down by cells, there is something specific about the surface of crystalline silica particles entering the uptake pathway that must cause toxicity.

There are several models that have been proposed for the molecular triggers that lead to cell death. One possibility is that when NADPH oxidase becomes activated on the phagosomal membrane, the presence of iron contaminating the silicon dioxide causes hydrogen peroxide to be converted to hydroxyl radicals by a Fenton reaction [5, 34]. Consistent with this hypothesis, iron chelators like desferrioxamine [21, 22, 34] and surface modifying agents like Polyvinylpyridine-N-oxide (PVPNO) or aluminum lactate [9, 12] have been shown to reduce cell death in crystalline silica exposed cells. Hydroxyl radicals could damage lysosomal membranes leading to permeabilization and leakage of fluorescent dextran into the cytoplasm. Our results show that phago-lysosomal membrane damage is an early event following crystalline silica uptake, occurring as early as 15 min after crystalline silica uptake. Using different molecular weight Fitc-dextrans we were able to show the

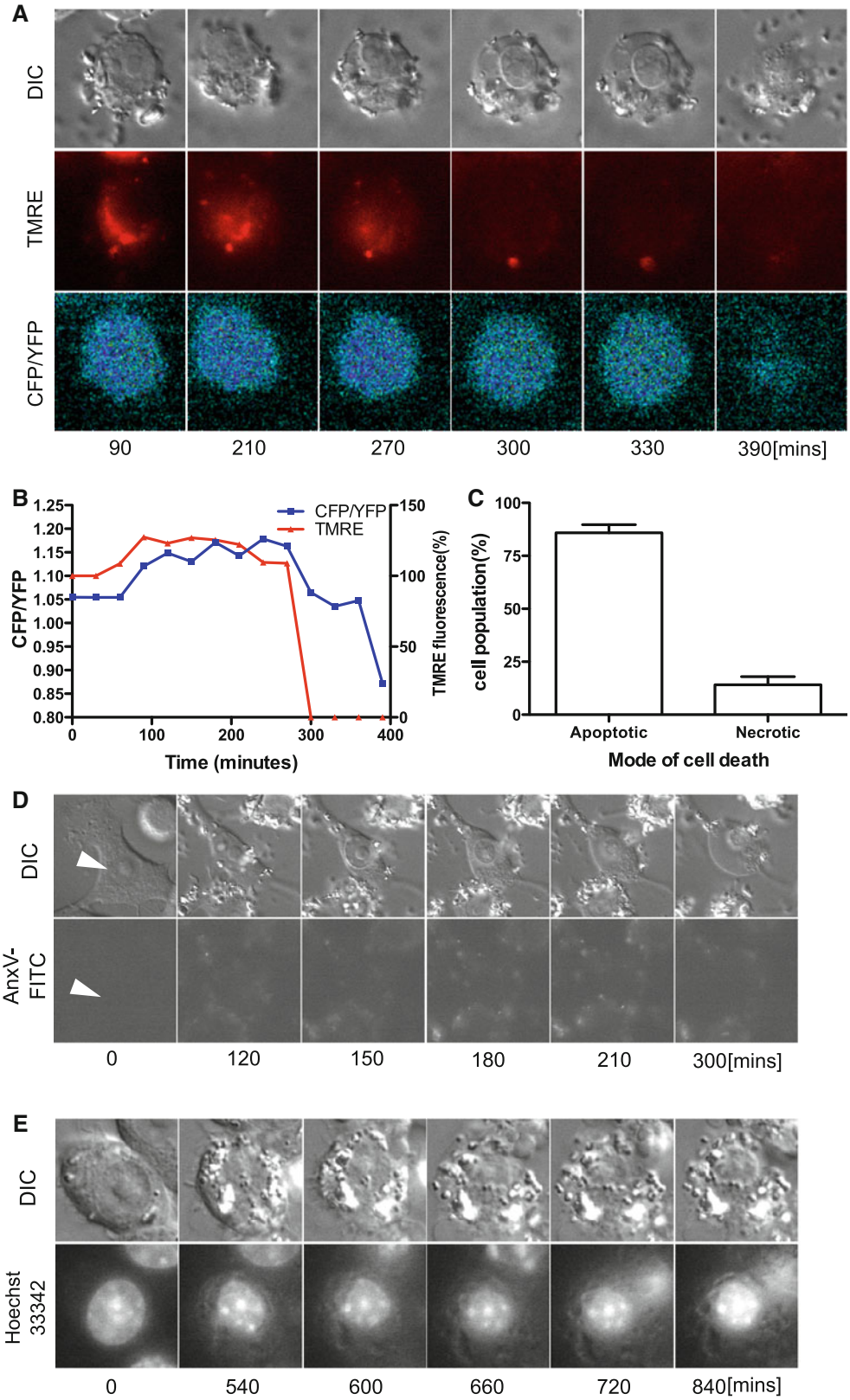

Fig. 7 Cells undergoing necrosis demonstrate mitochondrial depolarization without hyperpolarization and caspase activation. Some cells in the population undergo a distinct cell death process with hallmarks of necrosis rather than apoptosis. **a** Necrotic cells exhibit a swelling of cell membrane and nucleus with mitochondrial depolarization and no activation of the effector caspase as represented in the DIC, TMRE and the CFP/YFP images respectively. Similarly, for cells expressing the initiator caspase reporter probe there was no caspase activation observed (data not shown). **b** Quantitative analysis of these images show a decrease in TMRE fluorescence indicative of mitochondrial membrane depolarization during which there is no change in the FRET-ratio. **c** In cells expressing either of caspase reporter probes, approximately 15 % of cells exposed to crystalline silica die by necrosis and 85 % by apoptosis. Data of 444 cells from 12 separate experiments are shown as mean + S.E.M. Necrotic cells were identified by cell swelling (DIC) and then examined in the presence of either **d** Annexin V-FITC or **e** Hoechst 33342. Necrotic cells do not show either Annexin V-FITC membrane staining or nuclear condensation

release of molecules at least as large as 70 kD from phagolysosomes. The detection of leakage is aided by the fact that the fluorescence of dextran in the cytoplasm is much brighter than the vesicular dye due to the unquenching of the fluorescein when it moves from the low pH vesicular environment to the more neutral pH of the cytoplasm. Since

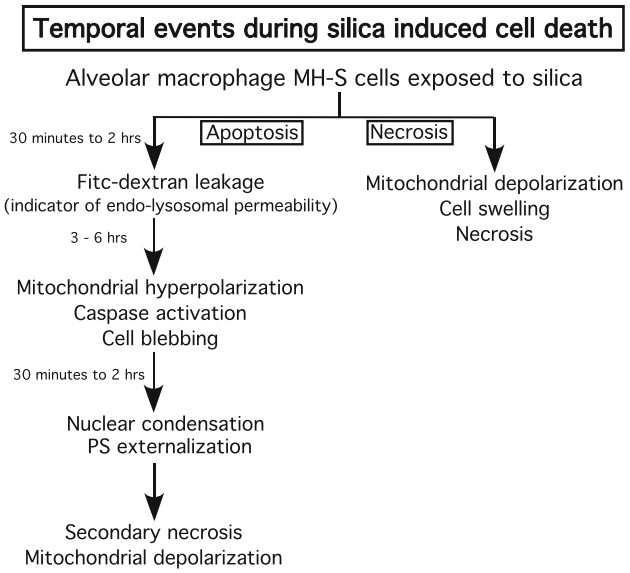

Fig. 8 Pathway showing temporal difference between each molecular event leading to cell death. A pathway of based on temporal variations in cell death summarizes the results from single cell analysis of different probes. Alveolar macrophages treated with crystalline crystalline silica die by either apoptosis or necrosis. 85 % of cells undergo apoptosis and show FD leakage as early as 30 min and lasting until 2 h after exposed to crystalline silica. After a long delay, cells begin apoptosis that is characterized by cell blebbing, mitochondrial hyperpolarization and caspase activation. These three events are tightly synchronized. Both PS externalization and nuclear shrinkage occur after 30 min–2 h after above-mentioned events followed by secondary necrosis and mitochondrial depolarization. The 15 % of cells undergoing necrosis show cell swelling characterized by mitochondrial depolarization. Caspase activation is not seen during this necrosis

molecules as large as 70 kD, and probably larger can pass through the membrane, the cytoplasmic milieu would be exposed to many enzymes and proteins normally restricted to the lysosome.

Exposure of macrophages to crystalline silica has been previously reported to cause phago-lysosomal leakage leading to inflammasome activation and IL1-β release [35–38]. In these studies, macrophages were always stimulated with lipopolysaccharide (LPS). Without LPS stimulation, high doses of crystalline silica failed to activate the NLRP-3 inflammasome, activate caspase-1 or cause IL1-β release [35, 36, 39]. In separate studies, monocytes and macrophages that were not pre-stimulated with LPS failed to activate caspase-1 in response to inflammasome activators [40, 41]. Since macrophages in our experiments were not pre-stimulated with LPS we are looking at events that occur independent of inflammasome activation.

Lysosomes contain cysteine proteases like cathepsins that are less than 50 kD in size and therefore can leak into the cytoplasm following membrane permeabilization [42]. Cathepsin inhibitors cause a reduction in apoptosis of crystalline silica treated macrophages [8]. Cathepsin in the cytoplasm is able to activate the pro-apoptotic protein Bid [42] resulting in mitochondrial outer membrane permeabilization (MOMP) by Bax [43] and cytochrome c release from mitochondria [42]. Although a temporal sequence from lysosomal leakage to caspase activation has not been demonstrated, our results show that the time lag from phago-lysosomal leakage to caspase activation was usually more than 3 h. This leaves a wide temporal gap between the proximal and late event during apoptosis.

Changes in mitochondrial membrane potential and caspase activation have been shown to be key indicators in apoptosis and a point of no return leading to cell death [44, 45]. Exposure to crystalline silica has been shown to lead to activation of both caspase-9 and -3 and mitochondrial depolarization but previous studies have not been able to resolve how the events relate temporally to each other. This is the first study of crystalline silica exposure where this question is resolved. Cells expressing either initiator or effector caspase (FRET) reporter probes along with TMRE show dramatic mitochondrial hyperpolarization that occurs simultaneously with cleavage of caspase FRET probes and cell membrane blebbing. Earlier studies have shown specificity of the individual FRET reporter probes towards their respective caspases [23, 24]. Based on the 5-min time interval between captured images, we can say that caspase activation, hyperpolarization and cell membrane blebbing occurred within 5 min of each other. Cleavage for FRET reporter probes and membrane blebbing continued for some time after hyperpolarization had ended. Although our study did not measure the rate of release of mitochondrial intermembrane space proteins like cytochrome c and Smac, other studies have shown the immediate release of these proteins upon MOMP [46, 47]. Furthermore, the duration of the cleavage of FRET probes is consistent with other studies [48]. Our study highlights the fact that the extended time of caspase activation as reported by the duration of cleavage of caspase reporter probes may not be necessary for downstream event like cell blebbing that happen within 5 min of initiation of cleavage and cannot be separated from the initiation of cleavage.

The observation that mitochondria go through a stage of hyperpolarization en route to apoptosis is novel. Most studies of apoptosis have found only mitochondrial depolarization. Mitochondrial hyperpolarization has been observed previously during T cell activation [49]. It is not surprising that this phenomenon was missed in earlier studies of crystalline silica induced apoptosis. Population average measures of mitochondrial potential (e.g. from a fluorimeter) would not detect transient changes in a small population of cells. Even flow cytometry would likely miss these events because it is transient and so only a small proportion of the cells would be hyperpolarized at any

time. One possibility that had to be eliminated is that the increase in fluorescence of TMRE was due to dye unquenching. TMRE has been shown to self-quench at high concentrations, so dilution of the dye can appear similar to hyperpolarization. The concentrations used in this study were 45 nM which is less than previous studies and well below the concentration at which self-quenching has been shown to occur (400 nM) [50]. In addition, the ability of TMRE to detect mitochondrial hyperpolarization at the concentration used in this study was tested by treating cells with a F_1–F_0 ATP'ase inhibitor, oligomycin [51, 52]. This compound causes an increase in $\Delta\Psi m$ by interfering with proton transport and causing a buildup of protons in the intermembrane space. Cells treated with oligomycin show a rapid increase in TMRE fluorescence indicating the expected increase in $\Delta\Psi m$ and confirming that the TMRE probe is sensitive to increases in membrane potential.

In models of the extrinsic pathway of apoptosis, where TNF-related apoptosis inducing ligand (TRAIL) and cycloheximide (CHX) were used to induce apoptosis, a rapid increase in FRET activation was observed for both initiator and effector caspases. The activation of initiator caspase-8 occurred 2–4 h after drug addition and before MOMP. The FRET increase for effector caspase-3 was found to occur at the same time as MOMP and the beginning of mitochondrial depolarization [19, 53]. In the case of staurosporine activation of the intrinsic pathway, mitochondrial depolarization, cytochrome c release and effector caspase activation were observed at about the same time [24, 53]. Thus for effector caspase activation in both intrinsic and extrinsic pathways, MOMP was found to be a common point. Studies with crystalline silica induced apoptosis have shown cytochrome c release indicative of MOMP and our data highlights that hyperpolarization and caspase activation occur simultaneously. Crystalline silica does not activate the extrinsic pathway, as it is not known to bind either TRAIL or TNF receptor. The scavenger receptors that crystalline silica has been hypothesized to interact with [54] are not known to activate the Death Inducing Signaling Complex (DISC) as caspase-8 activation has not been observed [8, 10]. Similarly, staurosporine activation of the intrinsic pathway, does not lead to caspase-8 activation [53]. These results suggest that crystalline silica induces apoptosis via the intrinsic pathway and can therefore be a useful model in understanding unexplored aspects of this mode of cell death.

Our data and other studies [47, 48, 55] show cell to cell variation in the timing and extent of caspase activation and other molecular events leading to cell death. We also see this variation in the expression of markers like surface phosphatidyl serine (PS) exposure and chromatin condensation. In spite of these intercellular temporal differences every cell follows a similar order of events in the activation pathway leading to death (Fig. 8). In receptor mediated cell death this variability has been attributed to the differences in the state of protein expression required for cell death [55]. Rehm et al. [56] saw sister cells upon mitotic division die with less temporal variation than unrelated cells.

Annexin V binding to the outer leaflet of the plasma membrane has been proposed by some studies to be an early marker of apoptosis [57–60] where as others suggested it to be downstream of caspase activation [61]. In T cells, PS exposure was downstream of mitochondrial hyperpolarization and caspase activation, however there was no correlation between hyperpolarization and caspase activation [49, 62]. Our time-lapse microscopy reveals crystalline silica treated macrophages become Annexin V positive about 70 min after they begin to bleb. Since caspase activation occurs at the same time as blebbing, it is clear that Annexin V staining is a late or terminal stage marker of apoptosis in crystalline silica induced apoptosis. Nuclear fragmentation has been demonstrated by the TUNEL assay in previous studies with crystalline silica [6, 11, 12, 63] but time-lapse microscopy using Hoechst as an indicator revealed nuclear shrinkage occurs only after blebbing had started. This result indicates that nuclear changes also occur at a late stage of apoptosis.

PS externalization for cells in vivo would act as a signal for the neighboring cells to engulf apoptotic cells. However, in this in vitro assay, cells undergoing apoptosis do not have a nearby healthy population to phagocytose them and therefore they undergo secondary necrosis [10, 64]. During secondary necrosis, cells that were apoptotic with high mitochondrial $\Delta\Psi m$, lost mitochondrial membrane potential and underwent plasma membrane swelling. This is in contrast to the 15 % of cells that directly underwent necrosis as a result of crystalline silica exposure. The necrotic cells underwent rapid mitochondrial depolarization and membrane swelling, but showed none of the specific markers of apoptosis. Recently pyroptosis has been described as another way that cells die and undergo swelling [21, 65]. Pyroptosis is an anti-microbial response to various bacterial pathogens like *Legionella, Salmonella, Shigella*, and *Yersinia* and requires caspase-1 activation [66, 67]. Since the MH-S macrophages used in our experiments were not exposed to either bacteria or pre-stimulated with LPS, they would not have activated caspase-1. Therefore, the non-apoptotic death we have observed is unlikely to be due to pyroptosis. There were no obvious differences in the morphology of these cells or their interaction with silica particles that would suggest why they did not undergo apoptosis.

Using cell blebbing as a reference point, temporal differences between different physiological activities within the cell can be compared. During apoptosis, phago-lysosomal leakage

started to occur within 30 min of exposure to crystalline silica particles, followed 3–6 h later by mitochondrial hyperpolarization, caspase activation and cell blebbing. The latter three events could not be temporally resolved from one another during imaging that was done 5 min apart. Approximately 30 min to 2 h after the initial apoptotic activation, nuclear condensation and PS exposure was observed. Post apoptosis, cells necrosed (secondary necrosis) during which they show membrane swelling. Some cells also died by necrosis during which mitochondria rapidly depolarized followed by cell swelling (Fig. 8). This establishes a timeline of events that clearly distinguishes the molecular events that take place in the two cell death pathways that occur in crystalline silica treated cells.

Acknowledgments We are thankful to Dr. Toru Kawanishi at NIHS, Japan and Dr. Gavin Welsh at University of Bristol, UK for their gift of Initiator and Effector FRET caspase probes. We are also thankful to Dr. Carol Norris at UConn microscopy facility for her assistance.

References

1. Ross MH, Murray J (2004) Occupational respiratory disease in mining. Occup Med (Oxford, England) 54:304–310
2. Pelucchi C, Pira E, Piolatto G, Coggiola M, Carta P, La Vecchia C (2006) Occupational silica exposure and lung cancer risk: a review of epidemiological studies 1996–2005. Ann Oncol 17: 1039–1050
3. Dauber JH, Rossman MD, Pietra GG, Jimenez SA, Daniele RP (1980) Experimental silicosis: morphologic and biochemical abnormalities produced by intratracheal instillation of quartz into guinea pig lungs. Am J Pathol 101:595–612
4. Gardner DE (1984) Alterations in macrophage functions by environmental chemicals. Environ Health Perspect 55:343–358
5. Borges VM, Lopes MF, Falcão H, Leite-Júnior JH, Rocco PRM, Davidson WF, Linden R, Zin WA, DosReis GA (2002) Apoptosis underlies immunopathogenic mechanisms in acute silicosis. Am J Respir Cell Mol Biol 27:78–84
6. Wang L, Antonini JM, Rojanasakul Y, Castranova V, Scabilloni JF, Mercer RR (2003) Potential role of apoptotic macrophages in pulmonary inflammation and fibrosis. J Cell Physiol 194:215–224
7. Borges VM, Falcão H, Leite-Júnior JH, Alvim L, Teixeira GP, Russo M, Nóbrega AF, Lopes MF, Rocco PM, Davidson WF, Linden R, Yagita H, Zin WA, DosReis GA (2001) Fas ligand triggers pulmonary silicosis. J Exp Med 194:155–164
8. Thibodeau M, Giardina C, Hubbard AK (2003) Silica-induced caspase activation in mouse alveolar macrophages is dependent upon mitochondrial integrity and aspartic proteolysis. Toxicol Sci 76:91–101
9. Thibodeau MS, Giardina C, Knecht DA, Helble J, Hubbard AK (2004) Silica-induced apoptosis in mouse alveolar macrophages is initiated by lysosomal enzyme activity. Toxicol Sci 80:34–48
10. Hu S, Zhao H, Al-Humadi NH, Yin XJ, Ma JKH (2006) Silica-induced apoptosis in alveolar macrophages: evidence of in vivo thiol depletion and the activation of mitochondrial pathway. J Toxicol Environ Health A 69:1261–1284
11. Shen HM, Zhang Z, Zhang QF, Ong CN (2001) Reactive oxygen species and caspase activation mediate silica-induced apoptosis in alveolar macrophages. Am J Physiol Lung Cell Mol Physiol 280:L10–L17
12. Fubini B, Hubbard A (2003) Reactive oxygen species (ROS) and reactive nitrogen species (RNS) generation by silica in inflammation and fibrosis. Free Radic Biol Med 34:1507–1516
13. Iyer R, Hamilton RF, Li L, Holian A (1996) Silica-induced apoptosis mediated via scavenger receptor in human alveolar macrophages. Toxicol Appl Pharmacol 141:84–92
14. Rimal B, Greenberg AK, Rom WN (2005) Basic pathogenetic mechanisms in silicosis: current understanding. Curr Opin Pulm Med 11:169–173
15. Saffiotti U (2005) Silicosis and lung cancer: a fifty-year perspective. Acta bio-med: Atenei Parmensis 76(Suppl 2):30–37
16. Delgado L, Parra ER, Capelozzi VL (2006) Apoptosis and extracellular matrix remodelling in human silicosis. Histopathology 49:283–289
17. Slee EA, Harte MT, Kluck RM, Wolf BB, Casiano CA, Newmeyer DD, Wang HG, Reed JC, Nicholson DW, Alnemri ES, Green DR, Martin SJ (1999) Ordering the cytochrome c-initiated caspase cascade: hierarchical activation of caspases-2,-3,-6,-7,-8, and -10 in a caspase-9-dependent manner. J Cell Biol 144:281–292
18. Goldstein JC, Muñoz-Pinedo C, Ricci J-E, Adams SR, Kelekar A, Schuler M, Tsien RY, Green DR (2005) Cytochrome c is released in a single step during apoptosis. Cell Death Differ 12:453–462
19. Albeck J, Burke J, Aldridge B, Zhang M, Lauffenburger D, Sorger P (2008) Quantitative analysis of pathways controlling extrinsic apoptosis in single cells. Mol Cell 30:11–25
20. Bossy-Wetzel E, Newmeyer DD, Green DR (1998) Mitochondrial cytochrome c release in apoptosis occurs upstream of DEVD-specific caspase activation and independently of mitochondrial transmembrane depolarization. EMBO J 17:37–49
21. Galluzzi L, Maiuri MC, Vitale I, Zischka H, Castedo M, Zitvogel L, Kroemer G (2007) Cell death modalities: classification and pathophysiological implications. Cell Death Differ 14(7):1237–1243
22. Berghe TV, Vanlangenakker N, Parthoens E, Deckers W, Devos M, Festjens N, Guerin CJ, Brunk UT, Declercq W, Vandenabeele P (2010) Necroptosis, necrosis and secondary necrosis converge on similar cellular disintegration features. Cell Death Differ 17:922–930
23. Kawai H, Suzuki T, Kobayashi T, Mizuguchi H, Hayakawa T, Kawanishi T (2004) Simultaneous imaging of initiator/effector caspase activity and mitochondrial membrane potential during cell death in living HeLa cells. Biochim Biophys Acta 1693: 101–110
24. Tyas L, Brophy VA, Pope A, Rivett AJ, Tavaré JM (2000) Rapid caspase-3 activation during apoptosis revealed using fluorescence-resonance energy transfer. EMBO Rep 1:266–270
25. Schneider CA, Rasband WS, Eliceiri KW (2012) NIH Image to ImageJ: 25 years of image analysis. Nat Methods 9:671–675
26. Fried H, Kutay U (2003) Nucleocytoplasmic transport: taking an inventory. Cell Mol Life Sci 60:1659–1688
27. Tait SWG, Green DR (2010) Mitochondria and cell death: outer membrane permeabilization and beyond. Nat Rev Mol Cell Biol 11(9):621–632
28. Vander Heiden MG, Chandel NS, Williamson EK, Schumacker PT, Thompson CB (1997) Bcl-xL regulates the membrane potential and volume homeostasis of mitochondria. Cell 91: 627–637
29. Perry S, Gelbard H (2011) Mitochondrial membrane potential probes and the proton gradient: a practical usage guide. Biotechniques 50:98–115
30. Pfau JC, Brown JM, Holian A (2004) Silica-exposed mice generate autoantibodies to apoptotic cells. Toxicology 195:167–176
31. Ghiazza M, Polimeni M, Fenoglio I, Gazzano E, Ghigo D, Fubini B (2010) Does vitreous silica contradict the toxicity of the crystalline silica paradigm? Chem Res Toxicol 23:620–629

32. Gilberti RM, Joshi GN, Knecht DA (2008) The phagocytosis of crystalline silica particles by macrophages. Am J Respir Cell Mol Biol 39:619–627
33. Costantini LM, Gilberti RM, Knecht DA (2011) The phagocytosis and toxicity of amorphous silica. PLoS ONE 6:e14647
34. Persson HL (2005) Iron-dependent lysosomal destabilization initiates silica-induced apoptosis in murine macrophages. Toxicol Lett 159:124–133
35. Dostert C, Petrilli V, Van Bruggen R, Steele C, Mossman BT, Tschopp J (2008) Innate immune activation through Nalp3 inflammasome sensing of asbestos and silica. Science 320: 674–677
36. Kuroda E, Ishii KJ, Uematsu S, Ohata K, Coban C, Akira S, Aritake K, Urade Y, Morimoto Y (2011) Silica crystals and aluminum salts regulate the production of prostaglandin in macrophages via NALP3 inflammasome-independent mechanisms. Immunity 34:514–526
37. Davis MJ, Swanson JA (2010) Technical advance: caspase-1 activation and IL-1β release correlate with the degree of lysosome damage, as illustrated by a novel imaging method to quantify phagolysosome damage. J Leukoc Biol 88(4):813–822
38. Hornung V, Bauernfeind F, Halle A, Samstad EO, Kono H, Rock KL, Fitzgerald KA, Latz E (2008) Silica crystals and aluminum salts activate the NALP3 inflammasome through phagosomal destabilization. Nat Immunol 9:847–856
39. Hornung V, Latz E (2010) Critical functions of priming and lysosomal damage for NLRP3 activation. Eur J Immunol 40: 620–623
40. Schumann RR, Belka C, Reuter D, Lamping N, Kirschning CJ, Weber JR, Pfeil D (1998) Lipopolysaccharide activates caspase-1 (interleukin-1-converting enzyme) in cultured monocytic and endothelial cells. Blood 91:577–584
41. Schroder K, Sagulenko V, Zamoshnikova A, Richards AA, Cridland JA, Irvine KM, Stacey KJ, Sweet MJ (2012) Acute lipopolysaccharide priming boosts inflammasome activation independently of inflammasome sensor induction. Immunobiology 217(12):1325–1329
42. Droga-Mazovec G, Bojic L, Petelin A, Ivanova S, Romih R, Repnik U, Salvesen GS, Stoka V, Turk V, Turk B (2008) Cysteine cathepsins trigger caspase-dependent cell death through cleavage of bid and antiapoptotic Bcl-2 homologues. J Biol Chem 283:19140–19150
43. Bidère N, Lorenzo HK, Carmona S, Laforge M, Harper F, Dumont C, Senik A (2003) Cathepsin D triggers Bax activation, resulting in selective apoptosis-inducing factor (AIF) relocation in T lymphocytes entering the early commitment phase to apoptosis. J Biol Chem 278:31401–31411
44. Green DR, Reed JC (1998) Mitochondria and apoptosis. Science 281:1309–1312
45. Schwartz S (1998) Cell death and the caspase cascade. Circulation 97:227
46. Muñoz-Pinedo C (2006) Different mitochondrial intermembrane space proteins are released during apoptosis in a manner that is coordinately initiated but can vary in duration. Proc Natl Acad Sci USA 103:11573–11578
47. Albeck J, Burke J, Spencer S, Lauffenburger D, Sorger P (2008) Modeling a snap-action, variable-delay switch controlling extrinsic cell death. PLoS Biol 6:e299
48. Rehm M, Dussmann H, Janicke RU, Tavare JM, Kogel D, Prehn JHM (2002) Single-cell fluorescence resonance energy transfer analysis demonstrates that caspase activation during apoptosis is a rapid process. Role of caspase-3. J Biol Chem 277:24506–24514
49. Perl A, Gergely P, Nagy G, Koncz A, Banki K (2004) Mitochondrial hyperpolarization: a checkpoint of T-cell life, death and autoimmunity. Trends Immunol 25:360–367
50. Ehrenberg B, Montana V, Wei MD, Wuskell JP, Loew LM (1988) Membrane potential can be determined in individual cells from the nernstian distribution of cationic dyes. Biophys J 53:785–794
51. Rego AC, Vesce S, Nicholls DG (2001) The mechanism of mitochondrial membrane potential retention following release of cytochrome c in apoptotic GT1-7 neural cells. Cell Death Differ 8:995–1003
52. Giovannini C, Matarrese P, Scazzocchio B, Sanchez M, Masella R, Malorni W (2002) Mitochondria hyperpolarization is an early event in oxidized low-density lipoprotein-induced apoptosis in Caco-2 intestinal cells. FEBS Lett 523:200–206
53. Hellwig CT, Kohler BF, Lehtivarjo AK, Düssmann H, Courtney MJ, Prehn JHM, Rehm M (2008) Real time analysis of tumor necrosis factor-related apoptosis-inducing ligand/cycloheximide-induced caspase activities during apoptosis initiation. J Biol Chem 283:21676–21685
54. Hamilton RF, Thakur SA, Holian A (2008) Silica binding and toxicity in alveolar macrophages. Free Radic Biol Med 44:1246–1258
55. Spencer SL, Gaudet S, Albeck JG, Burke JM, Sorger PK (2009) Non-genetic origins of cell-to-cell variability in TRAIL-induced apoptosis. Nature 459:428–432
56. Rehm M, Huber HJ, Hellwig CT, Anguissola S, Dussmann H, Prehn JHM (2009) Dynamics of outer mitochondrial membrane permeabilization during apoptosis. Cell Death Differ 16:613–623
57. Martin SJ, Reutelingsperger CP, McGahon AJ, Rader JA, van Schie RC, LaFace DM, Green DR (1995) Early redistribution of plasma membrane phosphatidylserine is a general feature of apoptosis regardless of the initiating stimulus: inhibition by overexpression of Bcl-2 and Abl. J Exp Med 182:1545–1556
58. Zhang G, Gurtu V, Kain SR, Yan G (1997) Early detection of apoptosis using a fluorescent conjugate of annexin V. Biotechniques 23:525–531
59. Santarelli L, Recchioni R, Moroni F, Marcheselli F, Governa M (2004) Crystalline silica induces apoptosis in human endothelial cells in vitro. Cell Biol Toxicol 20:97–108
60. Brumatti G, Sheridan C, Martin SJ (2008) Expression and purification of recombinant annexin V for the detection of membrane alterations on apoptotic cells. Methods 44:235–240
61. Goldstein JC, Waterhouse NJ, Juin P, Evan GI, Green DR (2000) The coordinate release of cytochrome c during apoptosis is rapid, complete and kinetically invariant. Nat Cell Biol 2:156–162
62. Banki K, Hutter E, Gonchoroff N, Perl A (1999) Elevation of mitochondrial transmembrane potential and reactive oxygen intermediate levels are early events and occur independently from activation of caspases in Fas signaling. J Immunol 162:1466
63. Wang L, Bowman L, Lu Y, Rojanasakul Y, Mercer RR, Castranova V, Ding M (2005) Essential role of p53 in silica-induced apoptosis. Am J Physiol Lung Cell Mol Physiol 288:L488–L496
64. Majno G, Joris I (1995) Apoptosis, oncosis, and necrosis. An overview of cell death. Am J Pathol 146:3–15
65. Galluzzi L, Vitale I, Abrams JM, Alnemri ES, Baehrecke EH, Blagosklonny MV, Dawson TM, Dawson VL, El-Deiry WS, Fulda S, Gottlieb E, Green DR, Hengartner MO, Kepp O, Knight RA, Kumar S, Lipton SA, Lu X, Madeo F, Malorni W, Mehlen P, Nuñez G, Peter ME, Piacentini M, Rubinsztein DC, Shi Y, Simon H-U, Vandenabeele P, White E, Yuan J, Zhivotovsky B, Melino G, Kroemer G (2012) Molecular definitions of cell death subroutines: recommendations of the nomenclature committee on cell death 2012. Cell Death Differ 19:107–120
66. Bergsbaken T, Fink SL, Cookson BT (2009) Pyroptosis: host cell death and inflammation. Nat Rev Microbiol 7:99–109
67. Franchi L, Eigenbrod T, Muñoz-Planillo R, Nuñez G (2009) The inflammasome: a caspase-1-activation platform that regulates immune responses and disease pathogenesis. Nat Immunol 10:241–247